Mansoura Engineering Journal

Volume 48 | Issue 6 Article 7

October 2023

# Critical Buckling Coefficient of Tapered Web Plate girder under Compression and Bending Stresses

Saad A. Yehia
*Lecturer in Department of Civil Engineering, Higher Institute of Engineering and Technology, Kafr El-Sheikh, Egypt*, saadyhy81@gmail.com

Ramy I. Shahin
*Lecturer in Department of Civil Engineering, Higher Institute of Engineering and Technology, Kafr El-Sheikh, Egypt*



## Recommended Citation

Yehia, Saad A. and Shahin, Ramy I. (2023) "Critical Buckling Coefficient of Tapered Web Plate girder under Compression and Bending Stresses," *Mansoura Engineering Journal*: Vol. 48 : Iss. 6 , Article 7.
Available at: https://doi.org/10.58491/2735-4202.3088

ORIGINAL STUDY

# Critical Buckling Coefficient of Tapered Web Plate Girders Under Compression and Bending Stresses

Saad Abouelela Yehia*, Ramy Ibrahim Shahin

Department of Civil Engineering, Higher Institute of Engineering and Technology, Kafr El-Sheikh, Egypt

**Abstract**

**The tapered girders were developed as a cost-effective solution to the problem of long-span building construction. These systems are very attractive from an economic viewpoint, combining wide spans, quick erection, and easy access to services between the shallow parts of the beam and the ceiling below. Elastic local buckling is one of several modes of failure that must be considered during the structure design. Although elastic local buckling has been studied for decades, there is still a need to develop quick and comprehensive procedures that will reduce product design time, particularly during the presizing stage. Most design codes have no specific provisions for the particular case of non-rectangular panels, stating that they may conservatively be treated as rectangular panels with a larger width. This paper presented an extensive numerical analysis to estimate the critical local buckling coefficient of two typologies for trapezoidal tapered steel web plate girders with simply supported end conditions. The considered loading conditions are compression and bending stresses. Moreover, the study identifies the relative importance of several parameters that influence the local buckling phenomenon, such as the tapering ratio of the panel, normalized plate length, and ratio of minimum and maximum compressive stresses. Numerical results are used to propose approximate closed-form expressions that can be used to compute the local buckling coefficient. In addition, the elastic local buckling coefficients obtained from the proposed formulas were compared with the buckling coefficient predicted by both AISC and ECP-LRFD specifications. The proposed formulas are also verified against results obtained from nonlinear numerical analysis based on the finite element technique. The results indicate that the proposed formulas are valid for directly estimating the critical local buckling coefficient of trapezoidal tapered steel web plates. However, it is worth noting that the AISC and ECP-LRFD specifications have been shown to provide conservative predictions when calculating the local buckling coefficient for trapezoidal tapered steel web plate girders under stress gradients.**

*Keywords:* Combined compression and bending stresses, Elastic local buckling coefficient, Optimization technique, Regression analysis, Stress gradient, Tapered plate, Trapezoidal plate

## 1. Introduction

Tapered plate girders or columns are required when the steel structures have long-span lengths or massive loads. In contrast, hot-rolled beams are either not strong enough, have too much inertia, or are too expensive. Tapered plate girders are made from welded plates to create a more practical element. Consequently, trapezoidal parts with various moments of inertia are created, where a web panel with a linearly varying depth generates this variable inertia (Mirambell and Zárate, 2000). Web-tapered members can construct to provide the optimum strength and stiffness with the least weight, making it more significant in areas with high moments and thicker in regions with high shear. As a result, the tapered plate girders saved an amount of material compared with rolled shapes (Diez et al., 2019), and the importance of research into the behavior of tapered web plates emerged. Fig. 1 displays the usage of tapered plates in steel constructions, such as beams of industrial buildings.

Received 13 June 2023; revised 12 August 2023; accepted 24 August 2023.
Available online 16 October 2023

* Corresponding author at: Department of Civil Engineering, Higher Institute of Engineering and Technology, Kafr El-Sheikh, 33511, Egypt. Fax: 047- 3278865.
E-mail address: saad_yehia@kfs-hiet.edu.eg (S.A. Yehia).

https://doi.org/10.58491/2735-4202.3088

*Fig. 1. Tapered structural elements.*

Various steel design standards, such as AASHTO (American Association of State Highway and Transportation Officials, 2010) and AISC (A ISC, 2010), are used to determine the axial, bending, and shear capacities of web-tapered members based on experimental and theoretical research on prismatic members (Brahim et al., 2020). For example, The AISC Design Guide 25 (Kaehler and White, 2011) presented the procedure for calculating the strength of tapered members under shear, normal, and moment loads. In addition, it determines the reduction factor for the axial local web buckling and the web bending buckling factor in the flexure compression region.

Researchers also developed several models to predict the behaviour of tapered members to obtain design formulas. Pope (1962) suggested a pioneer's first theoretical technique of tapered plate buckling. The theoretical technique investigates the buckling analysis of a tapered plate symmetrically in plan-form under uniform compressive loading on the parallel ends. Two cases are considered; different uniform loads and equal uniform stresses applied normally to the ends. On the experimental side, the earliest references that investigated the plate buckling effect on the tapered member's failure were conducted by Pawel et al. (Prawel et al., 1974). In the past, numerical techniques have been utilized extensively to calculate the buckling stresses of nonrectangular plates, especially for skew plates (Wang et al., 1992; York and Williams, 1995; Huyton and York, 2001). Based on the Rayleigh-Ritz and Galerkin methods, Saadatpour and his team (Saadatpour et al., 1998, 2002) developed a numerical approach for analyzing arbitrary quadrilateral plates with arbitrary boundary conditions. Eid (1957) presented the analysis of thin tapered plates using the finite difference method. Moreover, he proposed a numerical expression of the thin plates bending under a randomly distributed lateral load. Additionally, the results of thin tapered plates were compared with equivalent rectangular plates under the same loading conditions, as well as different loading conditions. Furthermore, the study explored the effect of buckling mode shape and half-wavelengths on the minimum critical buckling stresses. Šapalas (2010) studied the local tapered web stability under pure bending moment using a theoretical and finite element analysis utilizing a COSMOS FEM code. Additionally, he conducted a thorough simulation using a large domain of the second-moment area ratio to calculate a critical load multiplier and investigate the effects of relative slenderness, steel grade, and moment of inertia of beam ends on the local stability of tapered beams. Ibrahim et al. (Brahim et al., 2020) conducted an extensive numerical investigation to propose formulas for the critical buckling coefficient of the prismatic tapered web plate girders. The authors studied the effect of different boundary conditions (simply supported, flange restrained, and fixed supported edges) and various loading conditions (uniform compression, pure bending, and pure shear) on the critical buckling coefficient. The AISC specifications currently adopt the equation proposed by Pekoz (1986) to determine the critical buckling coefficient for simply supported rectangular plate subjected to combined normal and bending stresses. Furthermore, Ibrahim et al. (Brahim et al., 2020) modify the Pekoz formula to determine critical buckling coefficient for simply supported prismatic tapered plate subjected to combined normal and bending stresses. Moreover, Diez et al. (2019). Developed a numerical analysis of trapezoidal plates subjected to uniform compression with four different boundary ends to Propose a closed formula to calculate the local buckling coefficient for trapezoidal plates. Ibrahim et al. (2021) conducted an experimental program utilizing three specimens to investigate the axial compressive strength of prismatic unstiffened slender tapered steel web. Complying with AISC design standards, new techniques are suggested to estimate the effective width of the web. Higher width-to-thickness and tapering ratios are proven conservative for this technique, and a new correction factor was proposed to determine these conservative results. Abu-Hamd (Abu-Hamd and El Dib, 2016) developed an approximate empirical formula for tapered plates girder. This formula is based on the numerical results obtained from the FEM of steel tapered web subjected to shear and moment. Kucukler et al. (Kucukler and Gardner, 2018) suggested a simplified stiffness reduction method for the in-plane

analysis of the tapered plates by dividing the web member into prismatic elements. Ziemian et al. (Ziemian, 2010) proposed a numerical technique to investigate tapered beams' lateral buckling, considering the effect of initial stress and load eccentricity. Finally, the composite plates field has provided a significant result on the behaviour of local buckling for trapezoidal plates (Ashok and Pitchaimani, 2018; Kumar et al., 2019; Jiang et al., 2018) and an interesting new field of research proposed by Jing and coworkers (Jing et al., 2019) to determine buckling loads of orthotropic plates.

Most design codes need more provisions to determine the local buckling of nonrectangular plates, where they can be considered conservatively as rectangular plates with a larger width. Little attention has been focused in the literature on studying the elastic local buckling of trapezoidal tapered web plate girders under compression and bending stresses. The main objective of this paper is to provide an extensive finite element analysis to estimate the critical local buckling coefficient of two typologies for trapezoidal tapered steel web plates with simply supported end conditions. As its main contributions, the paper first provides a complete and clear picture of deformed shapes for trapezoidal tapered plates. Moreover, the regression analysis and optimization techniques were performed using MATLAB software for the results of the finite element models to propose a formulas for each topology. The study ignored the role of the flange in constraining the web, and the flange effect is close to the hinged state.

## 2. Material and methods

### 2.1. Problem statement

Two typologies of trapezoidal tapered web plate girders in a cartesian coordinate system are given in Fig. 2. The plate has a length a, a constant width "h" at the larger side, and a variable width "h1" at the smaller side with thickness "t". The plate is subjected to linearly varying in-plane loading in the longitudinal direction, and all its edges are simply supported in the out-of-plane direction. In other words, there is no lateral edge displacement perpendicular to the plate plane on all four edges.

This paper assumed the existence of two different typologies of trapezoidal tapered web plate girders for tapering ratio R $\geq$ 1.00, which are among the most commonly used types of tapered girders in steel construction. The fundamental differences between the two types are the stress state in the inclined flange (tension or compression), where

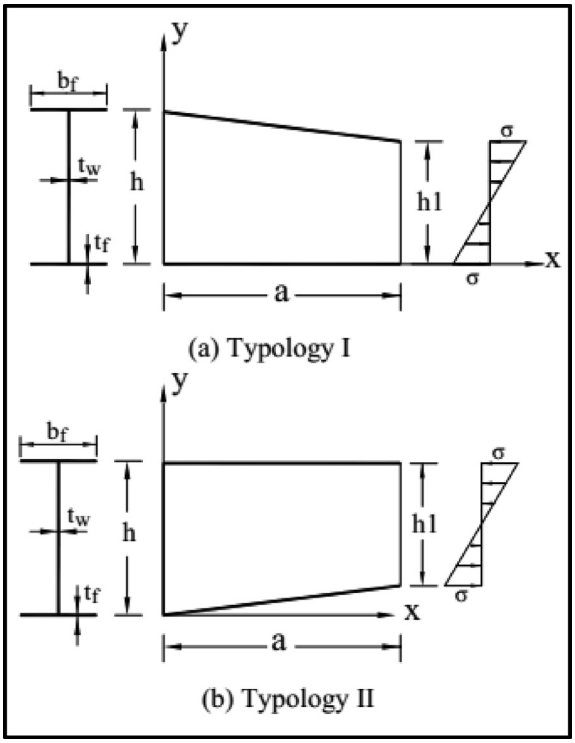


*Fig. 2. Geometry design parameters considered for two typologies of trapezoidal tapered web plate girders.*

typology I inclined flange under compression and typology II inclined flange under tension. The loading conditions are case (1) has a uniform compression load with $\Psi = 1$, case (2) has a trapezoidal load with $\Psi = 2/3$, case (3) has a trapezoidal load with $\Psi = 1/3$,case (4) has a triangular load with $\Psi = 0$, case (5) has an unequal reverse triangular load with $\Psi = -1/3$,case (6) has an unequal reverse triangular load with $\Psi = -2/3$, and case (7) has a pure bending load. for all compression and bending cases, nodal force is applied and divided according to different $\Psi$ ratios. Where, $\Psi$ is the ratio between minimum and maximum compressive stresses ($\Psi = \sigma_2/\sigma_1$) as shown in Fig. 3.

### 2.2. Finite element analysis procedure

For all study cases, the following steps were followed to develop predictive models:

(1) Choosing the inputs that may affect the critical buckling coefficient.
(2) The FE analysis using the ANSYS software (ANSYS, 2009) is used to execute an eigenvalue analysis to estimate the critical buckling load under normal and bending stresses. The

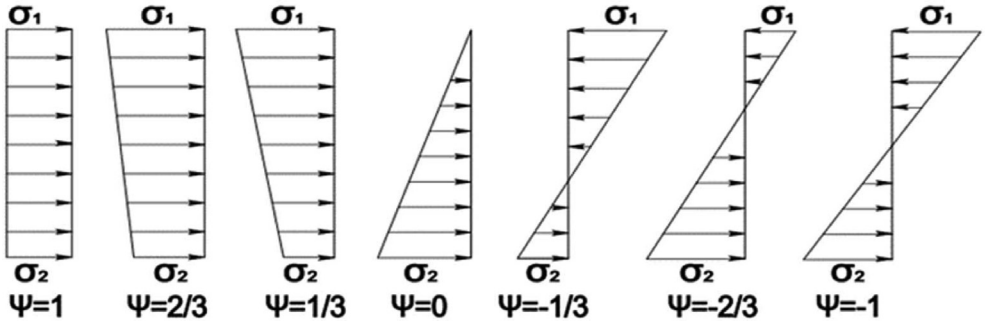


*Fig. 3. Example of in-plane loading conditions at x = a.*

program outputs are verified with well-known theoretical values;

(3) The elastic buckling coefficient is determined for each by using Timoshenko formula (Timoshenko and Gere, 1962).

(4) Construct the relations between the input variables and the predicted local buckling coefficient.

(5) Conducting a regression analysis to generate a predictive formula for design purposes.

### 2.3. Influencing parameters

Based on the literature reviews (Diez et al., 2019; Brahim et al., 2020; Pekoz, 1986), the fundamental parameters governing the predicted buckling coefficient are identified as the tapering ratio (R = h/h1), the normalized plate length ratio (α = a/h), the ratio of min. to max. Compressive stresses ($\Psi = \sigma_2/\sigma_1$) and loading and boundary conditions. according to Mirambell et al. (Mirambell and Zárate, 2000), the influence of the web depth-to-thickness ratio ($h / t_w$) is not significant, so the influence of this geometric parameter is ignored in this study. The parameter ranges and increments showed in (Table 1). The tapering ratio R ranges from 1 to 8. The normalized plate length α ranged from 0.25 to 8. The ratio of minimum to maximum compressive stresses ($\Psi = \sigma_2/\sigma_1$) equals 1,2/3,1/3,0, −1/3, −2/3, and −1 for compression and bending cases. The steel is modeled as a linear material with a Poisson ratio ν = 0.3 and modulus of elasticity E = 200 GPa.

### 2.4. Linear buckling analysis

Finite element analysis is performed using ANSYS engineering simulation software (ANSYS, 2009) with shell element to calculate the critical buckling load. A four-node shell element (SHELL181) is employed to model the tapered plate, which has six degrees of freedom at each node: translations in the x, y, and z directions and rotations about the x, y, and z-axes. In addition, SHELL181 is suitable for modeling thin to moderately thick shell structures, which enables explicit simulation of various buckling deformations. Buckling loads are obtained from eigenvalue analysis. Eigenvalue buckling analysis is also known as linear buckling analysis, where buckling load can be estimated by using the next equation (Chen et al., 2006).

$$([K_0] + \lambda[K_\sigma])\{U\} = 0 \quad (1)$$

where $K_o$ and $K_\sigma$ is the linear stiffness matrix and the geometric stiffness matrix, respectively. λ is the load scaling factor; {U} is the lateral displacement vector. From Eq. (1), it is clear that the structure's linear stability problem is the eigenvalue problem. By solving the eigenvalue and eigenvector problems, the critical load and buckling mode shape can be determined.

*Table 1. Different geometric of the parameter ranges and increments.*

| Studied parameter | Used parameter values for trapezoidal typology |
|---|---|
| | Compression and bending cases |
| Tapering ratio R (h/h1) | 1, 1.25, 1.5, 1.75, 2, 2.25, 2.5, 2.75, 3, 4, 5, 6, 8 |
| Normalized plate length α (a/h) | 0.25, 0.30, 0.35, 0.4, 0.45, 0.5, 0.55, 0.60, 0.65, 0.70, 0.75, 0.80, 0.85, 0.90,0 0.95 1.00, 1.05, 1.10,1.15, 1.20, 1.25,1.30, 1.35, 1.40, 1.45, 1.50, 1.55, 1.60, 1.65, 1.70 1.75, 1.80, 1.85, 1.90, 1.95, 2.00, 2 0.25, 2.50, 2.75, 3.00, 3.25, 3.50, 3.75, 4, 6, 7, 8 |
| The ratio between minimum and maximum compressive stresses ($\psi = \sigma_2/\sigma_1$) | 1,2/3,1/3,0, −1/3, −2/3, and −1 |

*Table 2. Numerical and theoretical results of critical buckling coefficient for tapered web plates with tapering ratio (R = 1.00).*

| Loading conditions | Normalized plate length (α = a/h) | Theoretical results Pekoz (Pekoz, 1986) | Numerical results this study (FEM) | Error % |
|---|---|---|---|---|
| (Uniform Compression (ψ = 1)) | 1 | 4.00 | 3.91 | 2.25 |
| | 2 | 4.00 | 3.947 | 1.325 |
| | 3 | 4.00 | 3.96 | 1.00 |
| | 4 | 4.00 | 3.967 | 0.825 |
| | 5 | 4.00 | 3.97 | 0.750 |
| (Trapezoidal Load (ψ = 1/3)) | 1 | 5.925 | 5.88 | 0.759 |
| | 2 | 5.925 | 5.90 | 0.422 |
| | 3 | 5.925 | 5.91 | 0.253 |
| | 4 | 5.925 | 5.916 | 0.152 |
| | 5 | 5.925 | 5.919 | 0.10 |
| (Triangle load (ψ = 0)) | 1 | 8.00 | 7.67 | 4.125 |
| | 2 | 8.00 | 7.70 | 3.75 |
| | 3 | 8.00 | 7.71 | 3.625 |
| | 4 | 8.00 | 7.723 | 3.465 |
| | 5 | 8.00 | 7.726 | 3.425 |
| (Unequal reverse triangular load (ψ = −1/3)) | 1 | 11.40 | 10.710 | 6.00 |
| | 2 | 11.40 | 10.745 | 5.70 |
| | 3 | 11.40 | 10.758 | 5.63 |
| | 4 | 11.40 | 10.760 | 5.63 |
| | 5 | 11.40 | 10.758 | 5.63 |
| (Unequal reverse triangular load (ψ = −2/3)) | 1 | 16.59 | 16.00 | 3.55 |
| | 2 | 16.59 | 15.88 | 4.28 |
| | 3 | 16.59 | 15.63 | 5.78 |
| | 4 | 16.59 | 15.57 | 6.14 |
| | 5 | 16.59 | 15.57 | 6.14 |
| (Pure bending (ψ = −1)) | 1 | 24.00 | 25.20 | 5.00 |
| | 2 | 24.00 | 23.87 | 0.54 |
| | 3 | 24.00 | 23.92 | 0.33 |
| | 4 | 24.00 | 23.82 | 0.75 |
| | 5 | 24.00 | 23.83 | 0.70 |

### *2.5. Validation of finite element model*

To guarantee the finite element model accuracy, a convergence test on mesh size has been carried out employing a reference to the exact theoretical values of the local buckling coefficient for supported rectangular plates (R = 1) (Pekoz, 1986). Table 2 provides the FEM error between the exact theoretical values of the local buckling coefficient and numerical results obtained from eigenvalue analysis, where used a mesh size (25*25 mm) for all loading cases. The normalized plate length ranged between 1 and 5. The last column of the table presents the error percentage, which varies from 0.10% to 6.14%. The comparison shows that the proposed boundary condition was well defined, and the results from the numerical are reasonable.

## 3. Results and discussions

### *3.1. Parametric study results and discussions*

Using the validated FE model, a parametric study that involved 9200 FE models was carried out for compression and bending loading cases to investigate the influence of the tapering ratio, normalized plate length, and the ratio of minimum to maximum compressive stresses Ψ equals (1,2/3,1/3,0, −1/3, −2/3, and −1) on the local buckling coefficient (Ziemian, 2010) for uniform compression load, trapezoidal compression load, triangle compression load, two unequal reverse triangular load cases, and pure bending, respectively. Fig. 4 shows the lowest deformed mode shape of trapezoidal tapered typologies for all compression and bending cases with simply supported boundary conditions.

Figs. 5 and 6 show the relationship between the plate buckling coefficients with normalized plate length (α) for several tapering ratios (R) of **typology I** and **typology II**, respectively, for uniform compression load (Ψ = 1), trapezoidal load (Ψ = 2/3), trapezoidal load (Ψ = 1/3), triangle load (Ψ = 0), unequal reverse triangular load (Ψ = −1/3), and unequal reverse triangular load (Ψ = −2/3) cases. It can be observed when the normalized plate length (α) is more than 1.00; the k values reduce with increasing (α) and R values. For α less than 1.00, buckling behavior is exactly the opposite, where k values

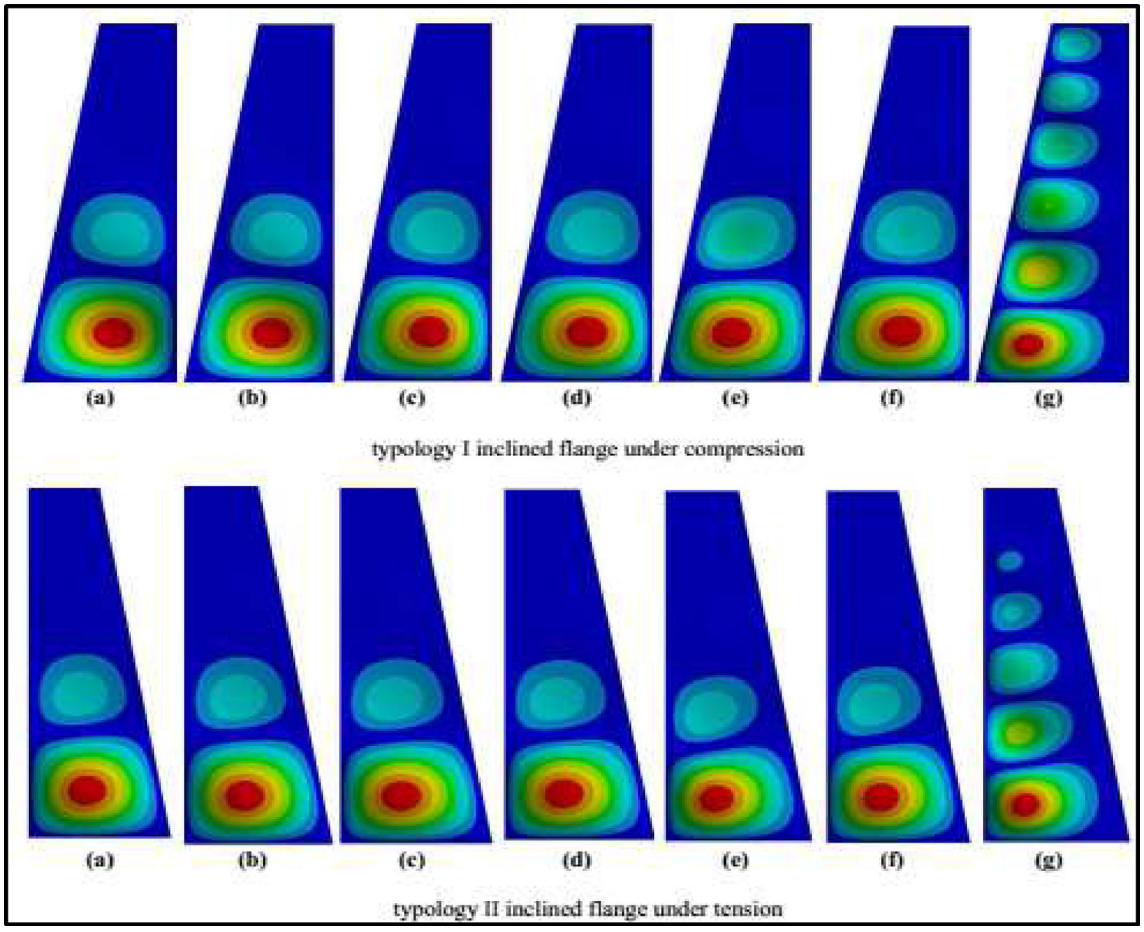


*Fig. 4. The lowest buckling mode of trapezoidal tapered typologies for (a) uniform compression load ($\psi = 1$) (b) trapezoidal compression load ($\psi = 2/3$) (c) trapezoidal compression load ($\psi = 1/3$) (d) triangle compression load ($\psi =$ Zero) (e) unequal reverse triangular load ($\psi = -1/3$) (f) unequal reverse triangular load ($\psi = -2/3$) (g) pure bending load (($\psi = -1$).*

increase with decrease $\alpha$ and decrease with increase R because the buckling waves are shorter when $\alpha$ values less than 1.00 compared with values more than 1.00. Moreover, for all R values, k declines with increases $\alpha$ up to 5.00, at which point the rate of decrease sharply declines. Typically, the applied stress along the loaded edges of plates ranges from uniform compression case to pure bending moment case. The uniform compression case is considered the most critical loading, and it has the lowest elastic local buckling stress. The parameter $\Psi$ ($\sigma_2/\ \sigma_1$) represents the varying stress distributions in a plate, where $\sigma_1$ is the maximum compressive stress and $\sigma_2$ is maximum tensile stress or minimum compressive stress. It can be noted that if the condition $\sigma_1 > 0$ is not satisfied, the Local buckling will not happen because the plate is subjected to only tension stress (Gardner et al., 2019).

Fig. 7 shows the relationship between the plate buckling coefficients with normalized plate length ($\alpha$) for several tapering ratios (R) of **typology I** and **typology II**, respectively of the pure bending load ($\Psi = -1$). It can be observed when the normalized plate length ($\alpha$) is more than 2.00, the predicated plate buckling coefficient values for all tapering ratios (R) values tend to reach 23.90 for simply supported edges. For the range of $\alpha < 2.00$ (hatched in Fig. 7), the critical buckling coefficient k values are noticeably lower than expected, especially for higher tapering ratios. Because the interaction with the induced shear stresses developed by additional shear force results from the vertical component of the flange force (Studer et al., 2015). So, it can be ignoring these deviations because they aren't in the practical application domain of these tapered plates.

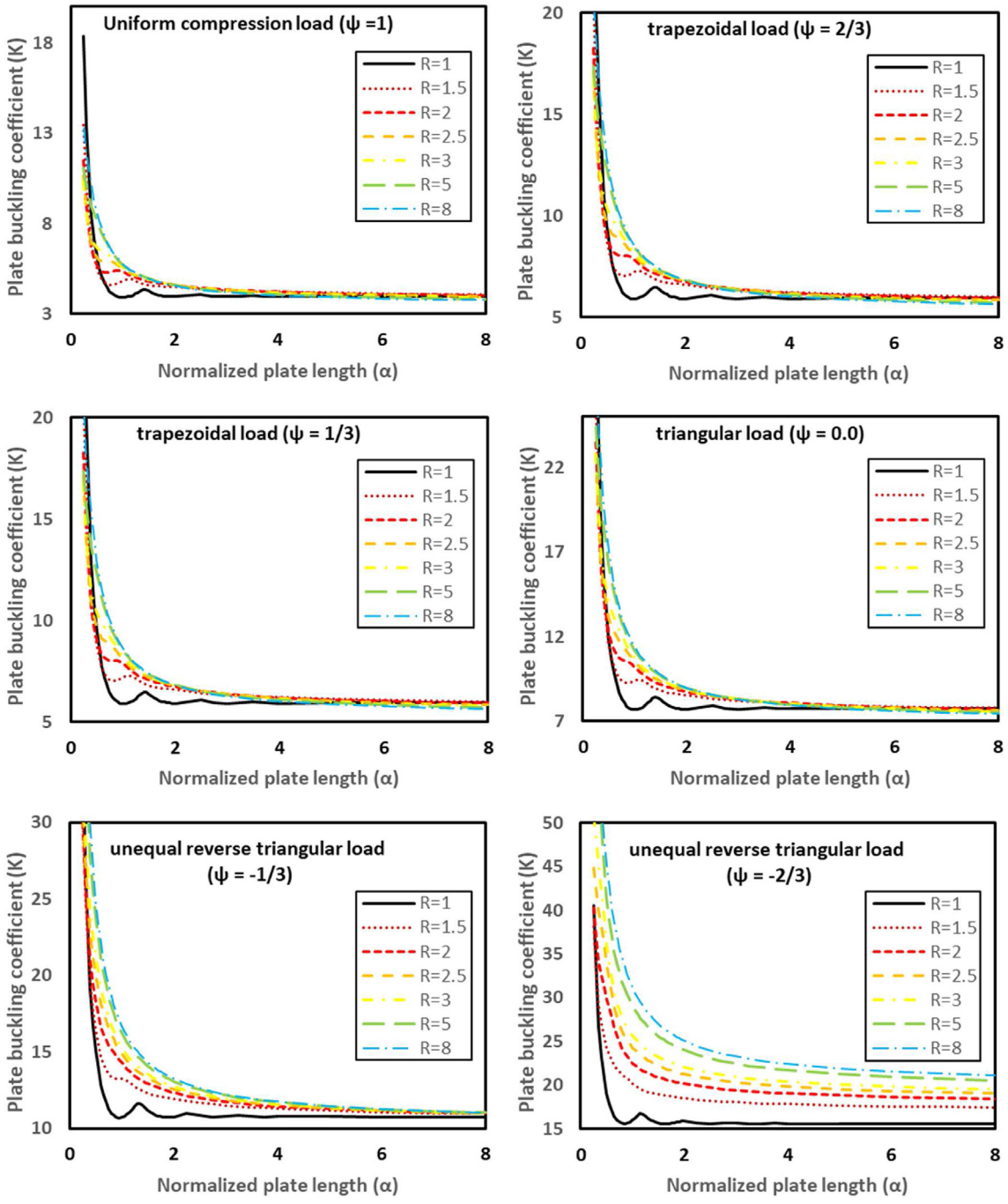


*Fig. 5. Plate buckling coefficient against normalized plate length (α) for several tapering ratios (R) of* ***typology I*** *for uniform compression load (ψ = 1), trapezoidal load (ψ = 2/3), trapezoidal load (ψ = 1/3), triangle load (ψ = 0), unequal reverse triangular load (ψ = −1/3), and unequal reverse triangular load (ψ = −2/3) cases.*

### *3.2. Proposed formulas of the elastic local buckling coefficients of trapezoidal tapered web plate girders under compression and bending stresses*

#### *3.2.1. Formulas for compression and bending cases*

A regression analysis is employed in the output results to propose a prediction of the critical buckling of tapered web subjected to compression and bending stresses. Regression analysis with MATLAB is performed to estimate the relation between the output (k) and inputs, including stress ratio (Ψ), normalized length (α), and tapering ratios (R). Moreover, regression analysis can measure the validity of predicted values with actual datasets

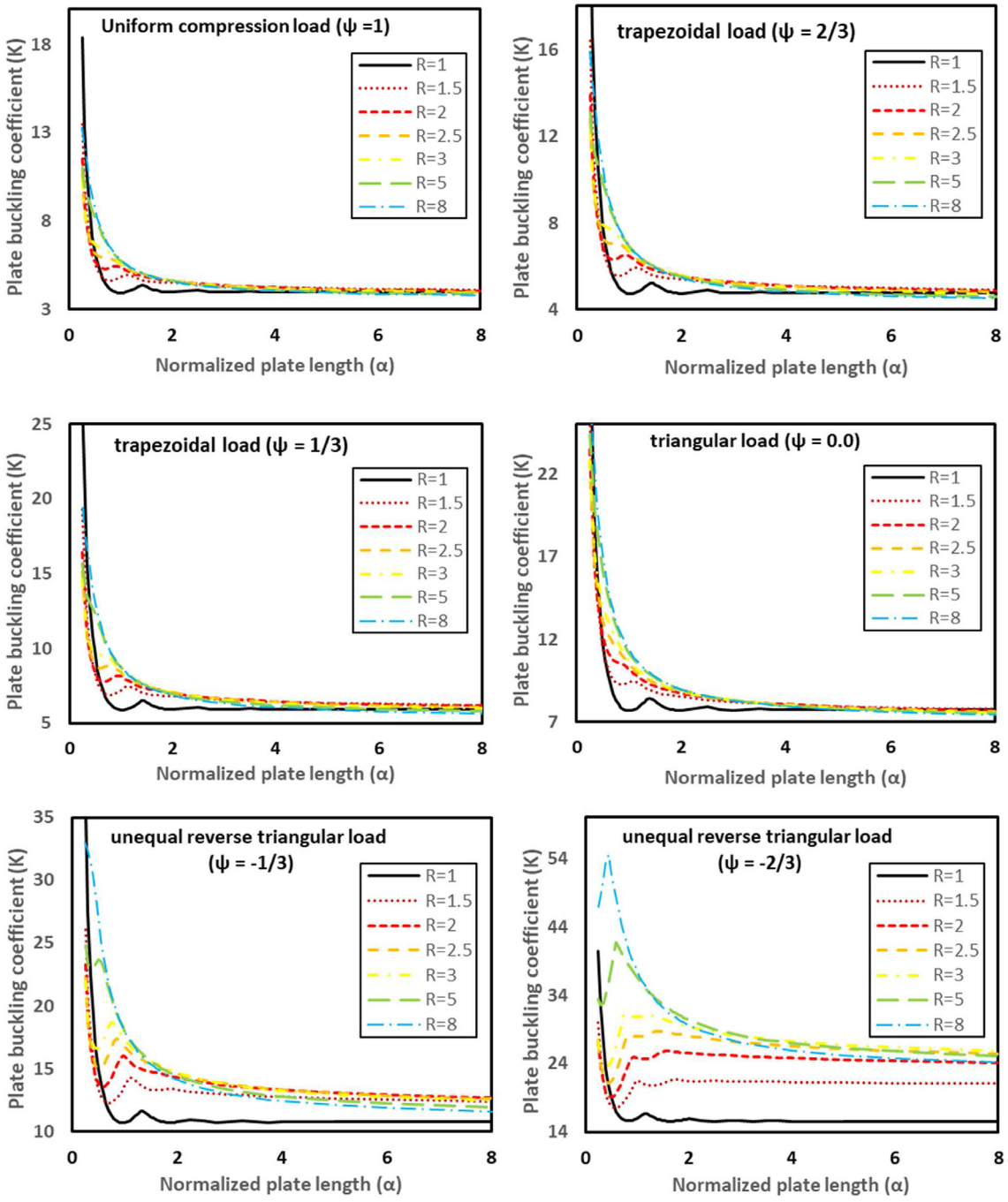


*Fig. 6. Plate buckling coefficient against normalized plate length (α) for several tapering ratios (R) of* ***typology II*** *for uniform compression load (ψ = 1), trapezoidal load (ψ = 2/3), trapezoidal load (ψ = 1/3), triangle load (ψ = 0), unequal reverse triangular load (ψ = −1/3), and unequal reverse triangular load (ψ = −2/3) cases.*

using many tools, such as coefficient of correlation (R), Mean Square Error (MSE), and Standard Deviation (SD). Table 3 shows the proposed buckling coefficient formulas for compression and bending stresses cases under simply supported boundary conditions of **typology I** and **typology II**.

### 3.2.2. Validation of proposed formulas

*Comparison with nonlinear numerical analysis based on the finite element technique*: The local buckling coefficients predicted by the proposed formulas were compared with the local buckling coefficients obtained from the finite element (FE) models of

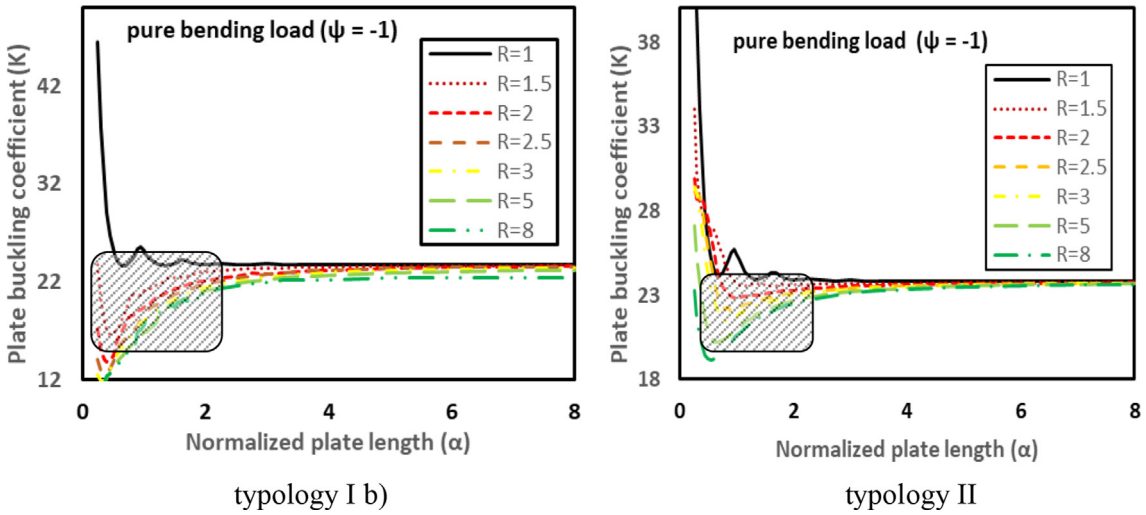


*Fig. 7. Plate buckling coefficient of pure bending load ($\psi = -1$) against normalized plate length ($\alpha$) for several tapering ratios (R).*

typology I and II, as shown in (Figs. 8 and 9). The comparison was made to all cases where $1 \leq \Psi \leq -1$. It can be noted that the mean values and the standard deviation ($\sigma$) values of the $K_{F.E}/K_{Prop.}$ ratio are (1.04 and 1.033) and (0.15 and 0.23) for **typology I and typology II**, respectively. Moreover, the coefficient of determination $R^2$ value is 0.953 and 0.930 for **typology I and typology II**, respectively, which indicates a very strong fit since it is close to 1. it can be noted that the proposed formulas provide a good prediction of the elastic buckling coefficient with high accuracy.

*Comparison with the design codes of practice*: For the case of combined bending and compression of a plate simply supported on all four sides. The American Institute of Steel Construction (AISC) specifications (A ISC, 2010) presented the following Eq. (2) to calculate the local buckling coefficient.

$$k = 4 + 2(1-\Psi)^3 + 2(1-\Psi) \quad (2)$$

Figs. 10 and 11 show a comparison between the local buckling coefficients obtained from the AISC formula and the local buckling coefficients obtained from the finite element (FE) models of typology I and II. The comparison was made to all cases where $1 \leq \Psi \leq -1$. It can be noted that the mean values and the standard deviation ($\sigma$) values of the $K_{F.E}/K_{ECP}$ ratio are (1.30 and 1.28) and (0.44 and 0.37) for **typology I and typology II**, respectively. Moreover, the coefficient of determination $R^2$ value is 0.893 and

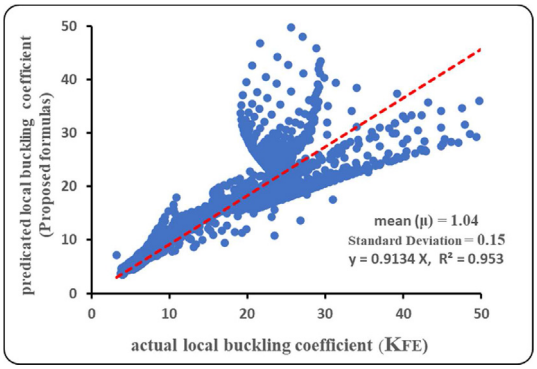


*Fig. 8. Comparison between the local buckling coefficients predicted by the proposed formulas and the local buckling coefficients obtained from the finite element (FE) models of typology I.*

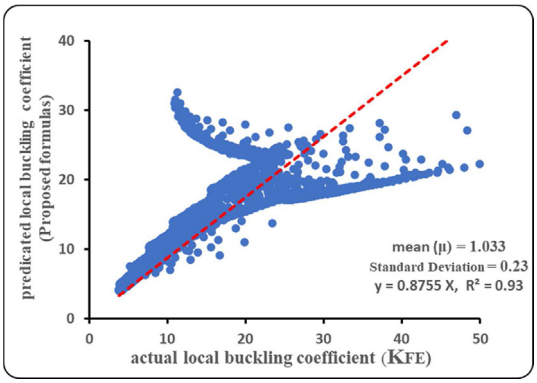


*Fig. 9. Comparison between the local buckling coefficients predicted by the proposed formulas and the local buckling coefficients obtained from the finite element (FE) models of typology II.*

*Table 3. Proposed buckling coefficient formulas for compression and bending stress cases under simply supported boundary conditions.*

| Typology number | Stress gradients | Buckling coefficient formulas |
|---|---|---|
| Typology I | $\psi = 1.00$ | $K_C = 0.27\alpha^{-2.3} - 15.65R^{0.4} + 20\alpha^{-0.022}R^{0.35}$ |
| | $1.00 > \psi \geq -1.00$ | $K_\sigma = -0.48 + 2.1C - 4.07\psi - 1.16\psi C + 4.9\psi^2$ Where, $C = 3.87 + 0.95\alpha^{-1.16}R^{0.36}$ |
| Typology II | $\psi = 1.00$ | $K_C = 3.862 + 1.03\alpha^{-1.064}R^{0.353}$ |
| | $1.00 > \psi \geq -1.00$ | $K_\sigma = 4.00 + 1.28K_C - 9.00\psi - 0.07\psi K_C + 3.95\psi^2$ |

Where, $K_C$ is the buckling coefficient at $\psi = 1.00$; C is constant; and $K_\sigma$ is the buckling coefficient at $1.00 > \psi \geq -1.00$.

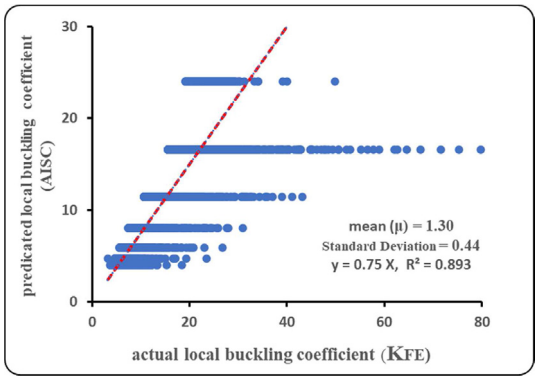


*Fig. 10. Comparison between the local buckling coefficients obtained from the AISC formula and the local buckling coefficients obtained from the finite element (FE) models of typology I.*

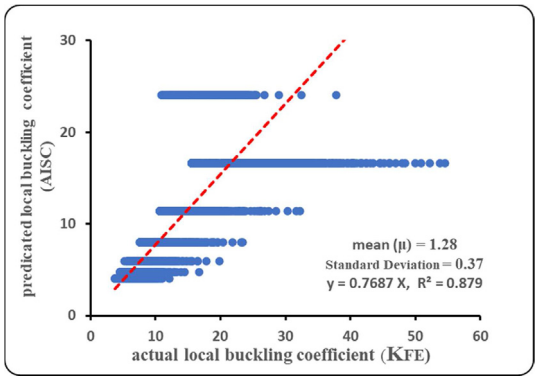


*Fig. 11. Comparison between the local buckling coefficients obtained from the AISC formula and the local buckling coefficients obtained from the finite element (FE) models of typology II.*

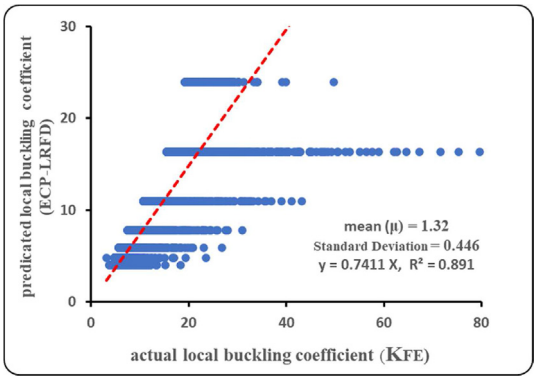


*Fig. 12. Comparison between the local buckling coefficients obtained from the ECP-LRFD formulas and the local buckling coefficients obtained from the finite element (FE) models of typology I.*

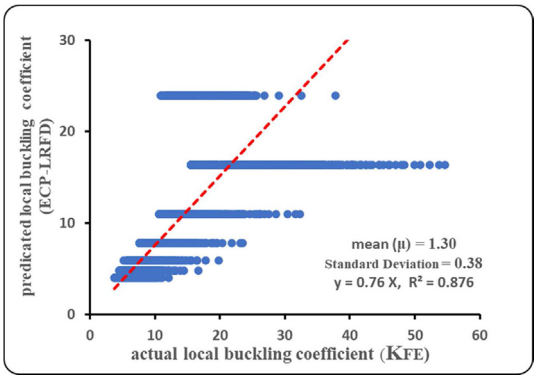


*Fig. 13. Comparison between the local buckling coefficients obtained from the ECP-LRFD formulas and the local buckling coefficients obtained from the finite element (FE) models of typology II.*

0.879 for **typology I and typology II,** respectively, which indicates a poor fit since it is close to 1.

Additionally, The elastic local buckling coefficients obtained from the F.E. models were compared with the local buckling coefficients predicted by the ECP-LRFD, 2008 (ECP-LRFD, 2008). The ECP-LRFD provides the following buckling coefficient formulas to calculate the local buckling coefficient, as shown in Table 4. Furthermore, it provides a single provision for tapered plates, which suggests that general design rules may be applied by assuming that the panel is rectangular with the maximum width

*Table 4. Buckling factor formulas for internal compression elements according to the ECP-LRFD, 2008.*

| Stress gradients ($\psi = \sigma_2/\sigma_1$) | Buckling factor $K_\sigma$ |
|---|---|
| $\psi = 1.00$ | 4.00 |
| $1.00 > \psi > 0.00$ | $8.2/(1.05 + \psi)$ |
| $\psi = 0.00$ | 7.81 |
| $0.00 > \psi > -1.00$ | $7.81 - 6.29\,\psi + 9.78\,\psi^2$ |
| $\psi = -1.00$ | 23.90 |

Figs. 12 and 13 show a comparison between the local buckling coefficients obtained from the ECP-LRFD, 2008 formulas and the local buckling coefficients obtained from the finite element (FE) models of typology I and II. The comparison was made to all cases where $1 \leq \Psi \leq -1$. It can be noted that the mean values and the standard deviation ($\sigma$) values of the $K_{F.E}/K_{ECP}$ ratio are (1.32 and 1.30) and (0.446 and 0.38) for **typology I and typology II,** respectively. Moreover, the coefficient of determination $R^2$ value is 0.891 and 0.876 for **typology I and typology II,** respectively, which indicates a very poor fit since it is close to 1.

After conducting comparisons, it has been demonstrated that both AISC and ECP-LRFD specifications are conservative when calculating the local buckling coefficient for trapezoidal plates under stress gradients. This is because these codes do not consider the significant impact of normalized

plate length and tapering ratio on the buckling coefficient. However, it is worth noting that the proposed formulas provide highly accurate predictions for the elastic buckling coefficient.

## 4. Summary and conclusions

This study presents a comprehensive finite element investigation into the structural behaviour for two different typologies of trapezoidal tapered web-girders under compression and bending stresses. More than 9200 models are employed to investigate the effect of several geomatic configurations, including the normalized plate length ratio ($\alpha$ = a/h), tapering ratio (R = $h/h_1$), and the ratio of minimum to maximum compressive stresses ($\Psi = \sigma_2/\sigma_1$) on the elastic critical buckling of the trapezoidal tapered web. The parameters range between the extreme values, keeping them in the practical range. The critical buckling coefficients are estimated for different compression and bending cases with simply supported boundary conditions, including uniform compression load, trapezoidal compression load, triangle compression load, two unequal reverse triangular load cases, and pure bending load. The regression analysis is employed to present a new formula for each case separately. Finally, statistical measurements were used to validate the research's proposed formulas such as correlation coefficient, mean square error, and standard deviation. Additionally, the elastic local buckling coefficients obtained from the proposed formulas were compared with the buckling coefficient predicted by both AISC and ECP-LRFD specifications. the main conclusions can be drawn as follow:

(1) Where the load is applied on the shorter edge, the buckling resistance of the tapered plate is directly proportional to the tapering of the web plate because the smaller edge provides a stiffer zone compared to the larger edge.
(2) The proposed formulas represent a significant improvement in predicting the critical buckling coefficient under compression and bending stresses and can be used to check web breathing in tapered web panels.
(3) For the pure bending moment case, it is recommended to ignore the decrease in k values for a tapering ratio of less than 2.00.
(4) The AISC and ECP-LRFD specifications have provided conservative predictions when calculating the local buckling coefficient for trapezoidal plates under stress gradients. However, the proposed formulas have been demonstrated to provide highly accurate predictions for the elastic buckling coefficient.

## 5. Recommendations for future work

When conducting future research, there are several essential matters that researchers should consider, such as:

(1) This paper presented an extensive numerical analysis to estimate the critical local buckling coefficient of two typologies for trapezoidal tapered steel web plate girder with simply supported end conditions; However, further researches may be required to identify other types of tapered girders such as prismatic tapered steel web plate girder.
(2) Further research may be required to identify the effect of other end conditions, such as fixed-free and fixed-hinge, in estimating the critical local buckling coefficient of tapered girders.
(3) Additionally, the study ignored the role of the flange in constraining the web, and the effect of the flange is close to the hinged state. This emphasizes the need for further research to investigate the impact of the flange on the local buckling coefficient of tapered girders.

## Author contribution

**Saad A. Yehia (Corresponding author):** Conceptualization, Methodology, Software, Validation, Formal analysis, Investigation, Data curation, Visualization, Project administration, Writing − original draft.

**Ramy I. Shahin:** Conceptualization, Methodology, Software, Validation, Formal analysis, Investigation, Data curation, Visualization, Writing − original draft.

### Conflicts of interest

The authors declare that they do not have any competing financial interests or personal relationships that could appear to have influenced the work reported in this paper.

## Acknowledgements

The author(s) received no financial support for the research and publication of this article.

## References


Aisc, 2010. 'Specification for Structural Steel Buildings'.

Abu-Hamd, M., el Dib, F.F., 2016. Buckling strength of tapered bridge girders under combined shear and bending. HBRC J 12, 163–174. https://doi.org/10.1016/j.hbrcj.2014.11.001.

American Association of State Highway and Transportation Officials, 2010. AASHTO LRFD Bridge Design Specifications. American Association of State Highway and Transportation Officials.

ANSYS, 2009. "Theory Manual, Swansea Company,".

Ashok, S., Pitchaimani, J., 2018. Buckling behavior of non-uniformly heated tapered laminated composite plates with ply drop-off. Int. J. Struct. Stabil. Dynam. 18, 4. https://doi.org/10.1142/S0219455418500591.

Brahim, M.M., El Aghoury, I.M., Ibrahim, S.A.B., 2020. 'Finite element investigation on plate buckling coefficients of tapered steel members web plates. Structures 28, 2321–2334. https://doi.org/10.1016/J.ISTRUC.2020.10.003.

Chen, N.-Z., Soares, C.G., Soares, C.G., Chen, N.Z., 2006. 'BUCKLING analysis of stiffened composite panels'. In: III European Conference on Computational Mechanics. Springer, Netherlands. https://doi.org/10.1007/1-4020-5370-3_686.

Diez, R., Lopez, C., Ibañez, J.R., Serna, M.A., 2019. Numerical study on elastic buckling and ultimate strength of compressed trapezoidal plates. Int. J. Struct. Stabil. Dynam. 20, 1. https://doi.org/10.1142/S0219455420500091.

ECP-LRFD, 2008. Egyptian Code of Practice for Steel Construction – Load and Resistance Factor Design LRFD. ' Ministry of Housing, Utilities and Urban development, Cairo, Egypt.

Eid, A., 1957. 'Ausbeulent Rapezfoermigen Platten' Ph.D. ETH, Zurich.

Gardner, L., Fieber, A., Macorini, L., 2019. Formulae for calculating elastic local buckling stresses of full structural cross-sections. Structures 17, 2–20. https://doi.org/10.1016/J.ISTRUC.2019.01.012.

Huyton, P., York, C.B., 2001. Buckling of skew plate a with continuity or rotational edge restraint. J. Aero. Eng. 14, 92–101.

Ibrahim, M.M., El Aghoury, I.M., Ibrahim, S.A.B., 2021. Experimental and numerical investigation of axial compressive strength of unstiffened slender tapered webs. J. Constr. Steel Res. 187, 106921. https://doi.org/10.1016/J.JCSR.2021.106921.

Jiang, G., Li, F., Zhang, C., 2018. Post buckling and nonlinear vibration of composite laminated trapezoidal plates. Steel Compos. Struct. 26, 17–29.

Jing, Z., Sun, Q., Liang, K., Chen, J., 2019. Closed-form critical buckling load of simply supported orthotropic plates and verification. Int. J. Struct. Stabil. Dynam. 19, 12. https://doi.org/10.1142/S0219455419501578.

Kaehler, R.C., White, D.W., 2011. Frame Design Using Web-tapered Members. AISC. Volume 25 of Steel design guide series.

Kucukler, M., Gardner, L., 2018. Design of laterally restrained web-tapered steel structures through a stiffness reduction method. J. Constr. Steel Res. 141, 63–76. https://doi.org/10.1016/j.jcsr.2017.11.014.

Kumar, A., Singha, M.K., Tiwari, V., 2019. Stability analysis of shear deformable trapezoidal composite plates. Int. J. Struct. Stabil. Dynam. 19, 8. https://doi.org/10.1142/S0219455419710044.

Mirambell, E., Zárate, A.V., 2000. Web buckling of tapered plate girders. Proc. Inst. Civ. Eng.: Struct. Build. 140, 51–60. https://doi.org/10.1680/STBU.2000.140.1.51.

Pekoz, T., 1986. Developement of a unified approach to the design of cold-formed steel members. Eighth Int Spec Conf Cold-Formed Steel Struct 77–84.

Pope, G., 1962. The Buckling of Plates Tapered in Planform. Aeronautical Research Council. R. & M. Nº. 3324.

Prawel, S.P., Morrell, M.L., Lee, G.C., 1974. Bending and buckling strength of tapered structural members. Weld Res Suppl 75–84.

Saadatpour, M.M., Azhari, M., Ma, Bradford, 1998. Buckling of arbitrary quadrilateral plates with intermediate supports using the Galerkin method. Comput. Methods Appl. Mech. Eng. 164, 297–306. https://doi.org/10.1016/S0045-7825(98)00030-9.

Saadatpour, M.M., Azhari, M., Ma, Bradford, 2002. Analysis of general quadrilateral orthotropic thick plates with arbitrary boundary conditions by the Rayleigh–Ritz method. Int. J. Numer. Methods Eng. 54, 1087–1102. https://doi.org/10.1002/NME.485.

Šapalas, V., 2010. Local stability of web of tapered beam subjected to pure bending. J. Civ. Eng. Manag. 16, 216–221. https://doi.org/10.3846/JCEM.2009.24.

Studer, R.P., Binion, C.D., Davis, D.B., 2015. Shear strength of tapered I-shaped steel members. J. Constr. Steel Res. 112, 167–174. https://doi.org/10.1016/J.JCSR.2015.04.013.

Timoshenko, S., Gere, J., 1962. Theory of elastic stability. J. Appl. Mech.

Wang, C.M., Liew, K.M., Alwis, W.A.M., 1992. Buckling of skew plates and corner condition for simply supported edges. J. Eng. Mech. 118, 651–662. https://doi.org/10.1061/(ASCE)0733-9399(1992)118:4(651).

York, C.B., Williams, F.W., 1995. Buckling analysis of skew plate assemblies: classical plate theory results incorporating Lagrangian multipliers. Comput. Struct. 56, 625–635. https://doi.org/10.1016/0045-7949(94)00568-N.

Ziemian, R.D., 2010. Guide to Stability Design Criteria for Metal Structures. John Wiley & Sons, Hoboken, NJ, USA.


*Title Arabic*

**معامل الإنحناء الحرج لعصب الكمرات المدببه تحت تاثير إجهادات الضغط والإنحناء**

*Arabic Abstract*


تستعرض هذه الدراسة تحليلا عدديا شاملا لتقدير معامل الإنحناء الحرج لعصب الكمرات المدببة والتي علي شكل شبة منحرف ذات الارتكاز البسيط تحت تاثير إجهادات الضغط و الإنجناء. وايضا حددت الدراسة عدة عوامل متغيرة وهي :نسبة التناقص في العصب ،ونسبة طول العصب الي عرضه، ونسبة الحد الأدنى الي الحد الأقصى لاجهادات الضغط والتي لها تاثير مهم في تقدير معامل الانحناء. تم إستخدام النتائج العددية لاقتراح عدة صيغ لحساب معاملات الإنحناء لجميع حالات التحميل المختلفه. اظهرت النتائج مدي دقه هذه الصيغ وسهوله استخدمها بطريقة مباشرة لحساب معامل الانجناء.